We are IntechOpen, the world's leading publisher of Open Access books
Built by scientists, for scientists

6,900
Open access books available

185,000
International authors and editors

200M
Downloads

154
Countries delivered to

Our authors are among the

TOP 1%
most cited scientists

12.2%
Contributors from top 500 universities

CLARIVATE ANALYTICS
BOOK CITATION INDEX
INDEXED

WEB OF SCIENCE™

Selection of our books indexed in the Book Citation Index
in Web of Science™ Core Collection (BKCI)

Interested in publishing with us?
Contact book.department@intechopen.com

Numbers displayed above are based on latest data collected.
For more information visit www.intechopen.com

Miniature Antenna with Frequency Agility

L. Huitema and T. Monediere

Additional information is available at the end of the chapter

http://dx.doi.org/10.5772/58838

1. Introduction

The need of both mobility and communication leads to the integration of antennas in miniature devices so far non-connected (particularly in medical areas). The dedicated volume for the antenna, including its ground plane, has to be kept at its acceptable minimum, involving low bandwidth. Moreover, due to their poor impedance bandwidth, small antennas tend to be very sensitive to the environment. Indeed, they are directly affected by their immediate surroundings, which disturb their working band, their radiation and their performances [1]. To counter the low bandwidth of the antenna and to adapt it to variable conditions and surroundings, it can integrate active components.

Thus, active components become highly suitable for the development of modern wireless communications. Indeed, they allow the miniaturization, shifting the antenna working frequency to be matched over a wide bandwidth by covering only the user channel and the adaptation of antennas to variable operating conditions and surroundings. It is in this framework that authors will propose in this chapter to detail the integration of active components in antennas to be more compact, smart and integrated.

The first part will address an overview of the most common used techniques for compact antennas to become active. In this goal, active antennas state-of-the-art will be presented:

- The first sub-section will present antennas integrating tunable components such as varactor diodes, MicroElectroMechanical systems (MEMS), Positive Intrinsic Negative (PIN) diode and Field Effect Transistor (FET).

- The second sub-section will focus on active antennas using tunable materials properties, i.e. ferroelectric materials and liquid crystal.

A second part will show relevant parameters for active antennas studies. It will exhibit both challenges and how to integrate active components in order to maximize the antenna per-

formances and efficiency. This part will be supported by concrete examples. Therefore, depending on their intended applications, readers will be prepared to find the best trade-offs between the agility method, the miniaturization and antenna performances.

The last part will be dedicated to present limitations of actual and most common solutions proposed for active and compact antennas. In this framework, new approaches will be detailed to overcome these physical limitations.

2. Overview of compact active antennas

Very small size antennas are needed for future dense wireless network deployment, for example in WBAN (Wireless Body Area Network) where the size is limited to dimensions much smaller (hearing aid, implants) than wavelength (λ_0=12.2 cm at 2.45GHz) or for the DVB-H (Digital Video Broadcasting – Handheld) application, where the miniaturization aspect is even more critical because it is a low frequency standard (λ_0=60 cm at 470 MHz). Therefore, the antenna has to be carefully optimized with trading off fundamental size limitations with its characteristics (especially bandwidth and efficiency). In addition, the environment of miniature antennas will be highly variable resulting in large antenna impedance and propagation channel changes. Several challenges have to be addressed. One of them is the adaptive antenna technology for compensating both low bandwidths and detuning effects.

The most commonly cited performance criterion is the achievable frequency tuning range (TR) defined as:

$TR(\%) = \dfrac{2(f_{max} - f_{min})}{f_{max} + f_{min}}.100$ where f_{max} and f_{min} are respectively the upper and the lower antenna operating frequency. The frequency tuning can either be continuous or discrete. The continuous frequency tuning is able to continuously cover each channel of a same standard while the discrete frequency tuning can only switch between different standards. This part will present the most common methods to target frequency tunable antennas design.

2.1. Integration of active components

2.1.1. Varactor diodes

For continuous frequency tuning, the integration of varactor diodes within an antenna is the most common approach [2-5]. P. Bhartia et al. were the first to publish antenna integrating varactor diodes [6]. Indeed, they presented a microstrip patch antenna with varactor diodes at the edges of the structure, as illustrated Figure 1. Both rectangular and circular tunable patches were studied, results reveal that 22% and 30% of bandwidth can respectively be achieved by varying the DC-bias-voltage between 0V and 30V.
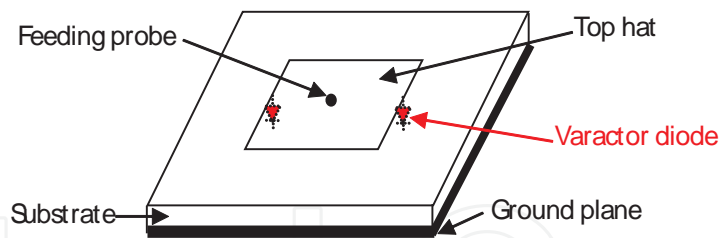
Figure 1. Patch antenna integrating varactor diodes [28]

Slot antennas are also good candidates for the frequency agility [7-9]. N. Behdad and K. Sarabandi presented in [9] a dual band reconfigurable slot antenna. The schematic of its proposed dual-band slot antenna is shown in Figure 2. Matching is performed by choosing appropriately the location of the microstrip feed and the length of the open circuited line.
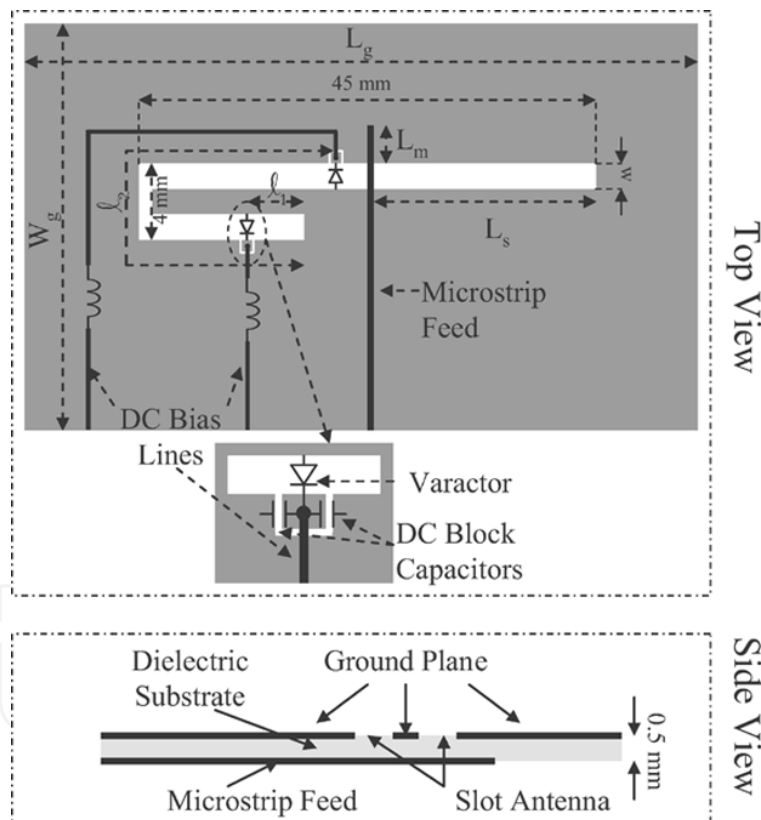

Figure 2. Dual reconfigurable slot antenna [9]

Figure 3 shows the simulated and measured dual-band responses of the antenna where by applying the appropriate combination of bias voltages (V_1 and V_2) the frequency of the first band is kept fixed and that of the second band is tuned. Similarly, as shown in Figure 3, it is possible to keep the frequency of the second band stationary and sweep the frequency of the first band.
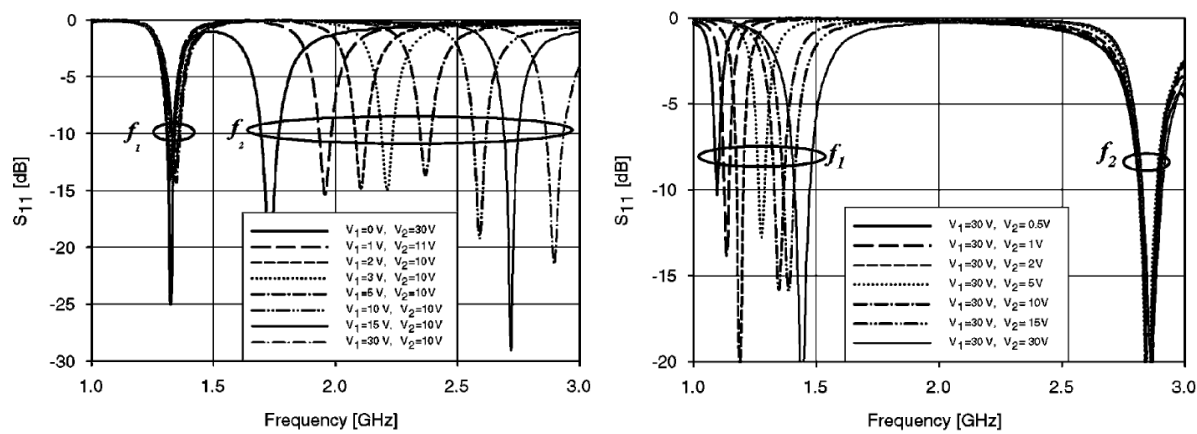
Figure 3. Measured $|S_{11}|$ parameters for different combination of bias voltages [9]

Another example show a 3D Inverted F Antenna [10] designed to cover the entire DVB-H band going from 470 MHz to 862 MHz. To be integrated in a mobile handheld device, the antenna allocated volume had to be very compact. A good trade-off between small sizes and the impedance bandwidth was to choose a structure based on the IFA design. Indeed, the radiating monopole of this kind of structure can be folded all around a material to become more compact (see Figure 4).
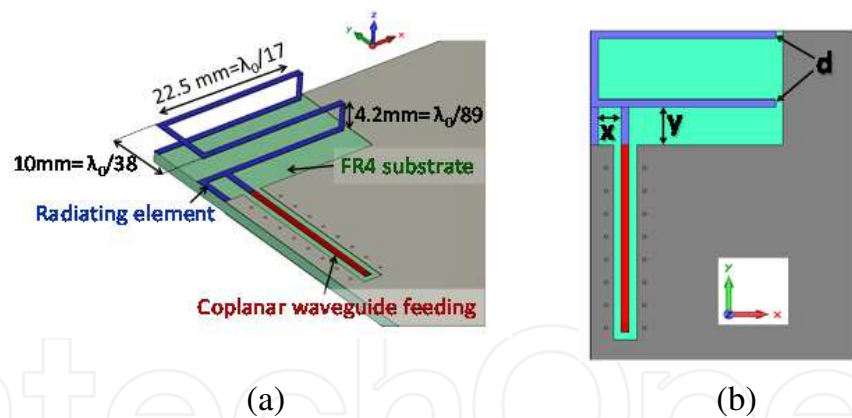

(a)   (b)

Figure 4. Inverted F Antenna design (a). Antenna top view (b) [10]

However, the more compact the antenna is, the lowest the bandwidth is becoming. To counter this issue, it has been proved that using a magneto-dielectric material rather than a dielectric one allows enhancing the input impedance bandwidth. Basing on this antenna design, the idea was to integrate a varactor diode to tune the impedance matching all over the DVB-H band (see Figure 5).

A prototype of the tunable antenna has been realized (Figure 6) and measured. For the diode polarization, a DC bias Tee is optimized with SMD components and measured on the DVB-H band (Figure 6). After being validated, it is integrated upstream from the antenna structure as
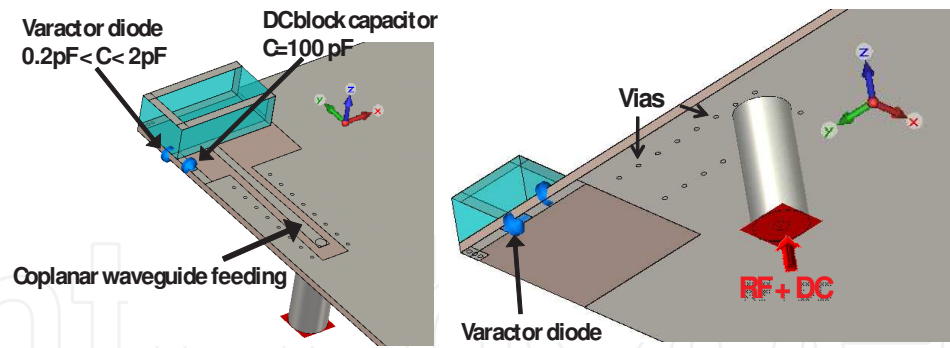
Figure 5. Design integrating both magneto-dielectric material and a varactor diode [10]

shown Figure 6. In order to improve the quality and the reliability of wireless links, the final mobile device is integrating two antennas (see Figure 6) for diversity operations.
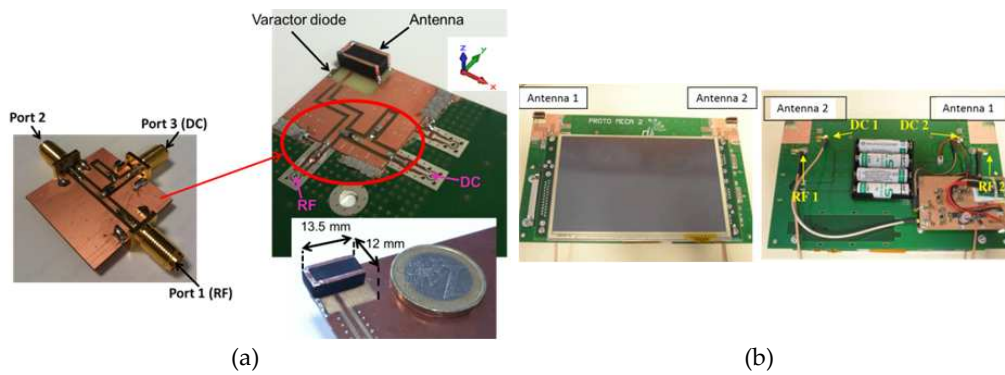

Figure 6. DC bias Tee with SMD components and its integration upstream from the antenna (a), integration of two antennas in the tablet dedicated to the DVB-H reception (b) [10]

Figure 7 presents respectively the variation of the input impedances and $|S_{11}|$ parameters of the antenna versus frequency for different values of the varactor diode bias voltages.
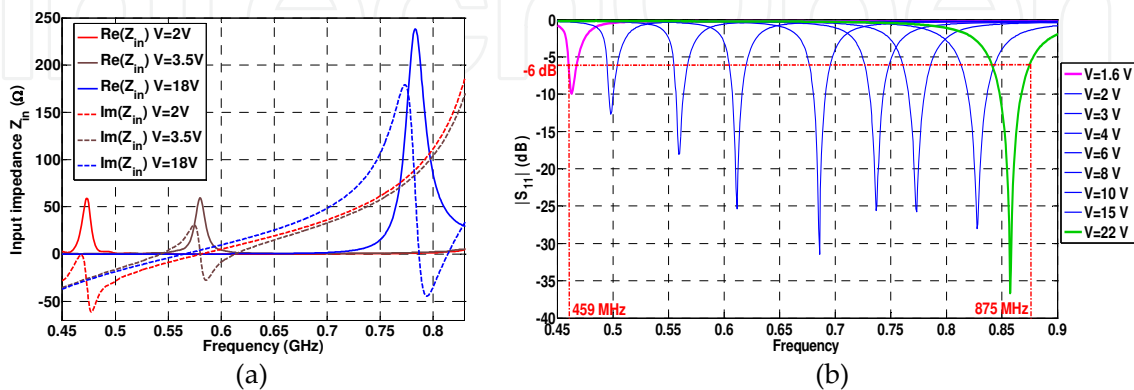

Figure 7. Measured input impedances (a) and $|S_{11}|$ parameters (b) for several DC bias voltages [10]

Therefore, the antenna working band is continuously tuned all over the whole DVB-H band. In the worst case, i.e. for a 2V DC bias voltage, the antenna is matched with $|S_{11}|$ <-6dB in a bandwidth which is covering more than one channel of the DVB-H band at-6 dB (largely suitable for the DVB-H standard).

2.1.2. Positive Intrinsic Negative (PIN) diodes

PIN diodes are using as switches:

- The ON state of the diode can be modelled by a zero resistance, i.e. a continuous metal strip across the slot where the diode is integrated.

- The OFF state of the diode can be modelled as an infinite resistance. The radiating length after the diode is not seen from RF point of view. The effective length of the antenna, and hence its operating frequency, is changing compared with the ON state case.

Selected antenna's types for integrating PIN diodes are often slot antennas or printed antennas (e.g. printed monopole, Inverted F Antenna, …). J-M. Laheurte presented in [11] a slot antenna including pin diodes for multi-frequency operation within a frequency octave.
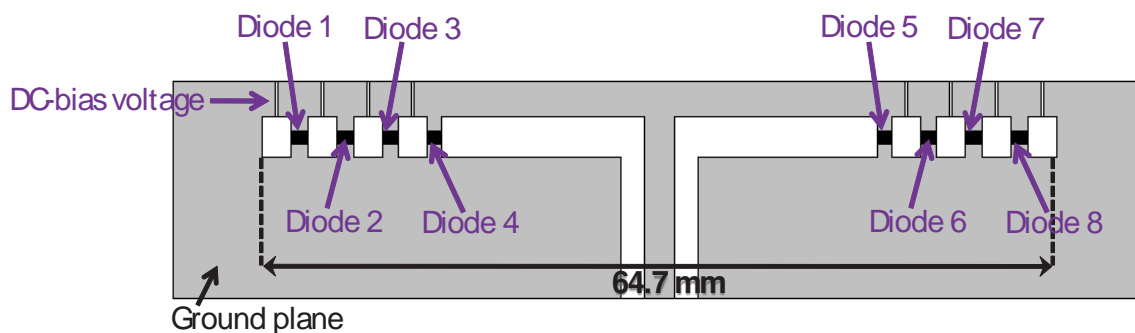

Figure 8. Switchable slot antenna including eight pin diodes [11]

As shown Figure 8, this antenna integrates eight PIN diodes and according to their ON or OFF states combination, the antenna can operate at different and discrete frequency bands (see Figure 9). Instantaneous impedance bandwidths are between 8% and 21% depending on the diodes' states combination.

Eventually, this antenna presents somewhat large dimensions since its main size is higher than à $\lambda_0/2$ at 2.8 GHz. The literature presents smaller antennas integrating PIN diodes since their main size are lower than à $\lambda_0/2$ at the working frequency [12].

Peroulis et al. [13] presented a tunable single-fed S-shaped slot loaded with a series of four PIN diodes. The effective length modification allows this antenna to operate in one of four selectable frequency bands between 530 and 890 MHz.

Before directly studying the tunable slot antenna, both single S-shaped slot antenna and PIN diodes were separately presented and studied. By this way, the issue related to the design of
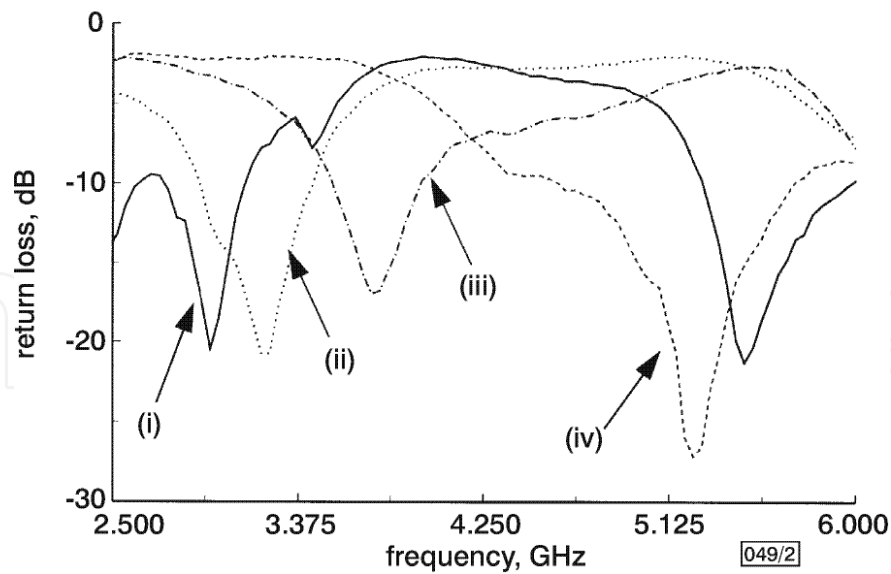
Figure 9. Measured $|S_{11}|$ parameters for different states of diodes: all diodes OFF (i), diodes 1, 8 ON (ii), diodes 1, 2, 7, 8 ON (iii) and diodes 1, 2, 3, 6, 7, 8 ON (iv) [11]

a suitable PIN switch has been grasped before integrate it and show its effects on the antenna performances. Indeed, to implement the electronic reconfigurability, the ideal shunt switches must be replaced by real PIN diodes. Therefore, the RF equivalent circuit of the diode has been studied (see Figure 10) for both the ON and OFF states. The reactive components C_p and L_p are modeling the packaging effect, while the others come from the electric properties of the diode junction in the ON and OFF positions. Then, the switch bias network was presented as an inductor of 470 nH and three 10 pF capacitors (Figure 10).
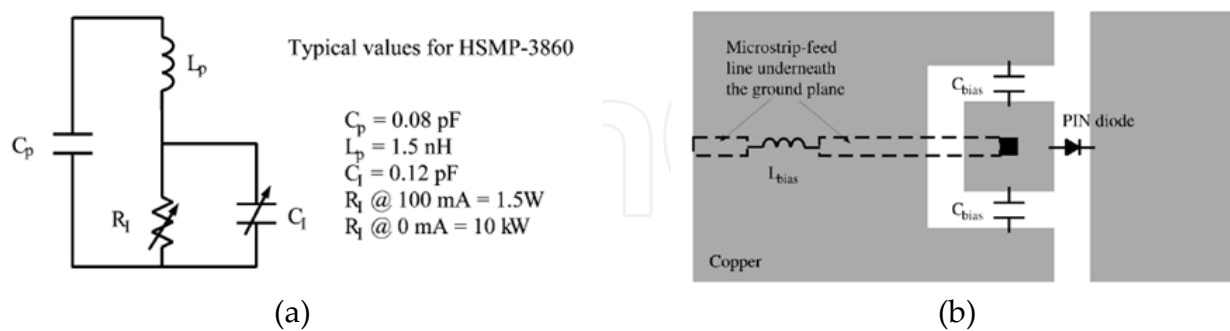

(a)   (b)

Figure 10. RF equivalent circuit of the PIN diode (a) and the switch bias network (b) [13]

Finally, a reconfigurable slot antenna design (Figure 11) is presented in this paper. Four switches are used in order to tune the antenna over a range of 540–950 MHz. The integration of the fours PIN diodes allows choosing the operating frequency of the antenna (Figure 11).
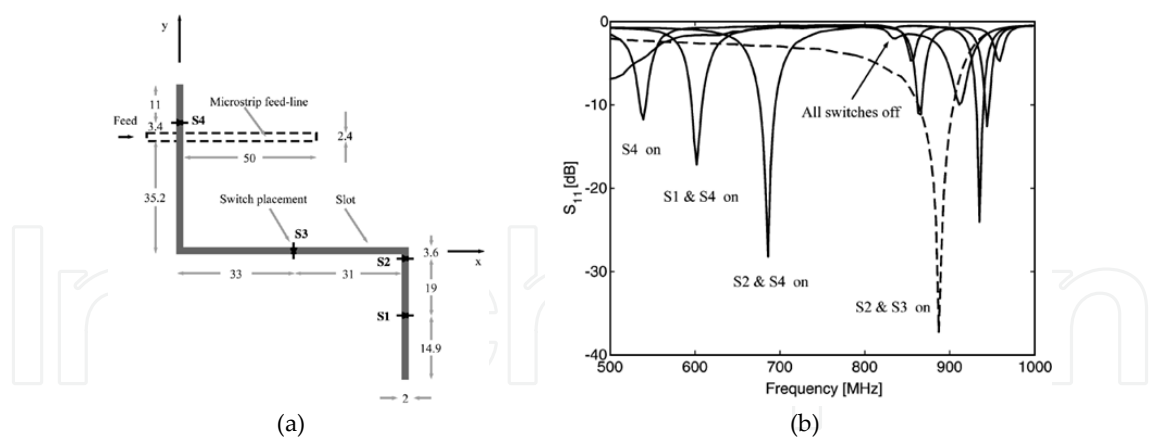
Figure 11. Reconfigurable slot antenna (a) and its measured |S$_{11}$| parameters (b) [13]

2.1.3. MicroElectroMechanical systems (MEMS)

MEMS components can allow:

- Continuous frequency tuning when they are used as a variable capacitance.

- Discrete frequency tuning, when they are used as switches.

E. Erdil presents in [14] a reconfigurable microstrip patch antenna integrating RF MEMS capacitor for continuously tuning the resonant frequency (see Figure 12). The reconfigurability of the operating frequency is obtained by loading one of the radiating edges of the microstrip patch antenna with a CPW stub on which RF MEMS bridge type capacitors are periodically placed.
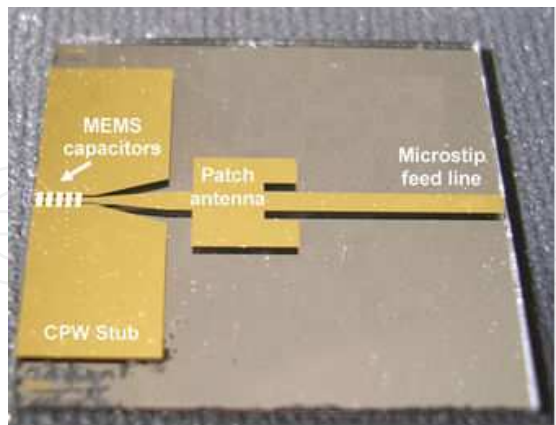

Figure 12. Frequency tunable microstrip patch antenna integrating MEMS capacitors [14]

When a DC voltage is applied, the height of the MEMS bridges on the stub is varying, and thus the loading capacitance is also changing. Therefore, as showed Figure 13 the matching frequency around 16.05 GHz shifts down to 15.75 GHz as the actuation voltage is increased from 0 to 11.9 V, where the height of the capacitive gap changes from 1.5 μm to 1.4 μm.
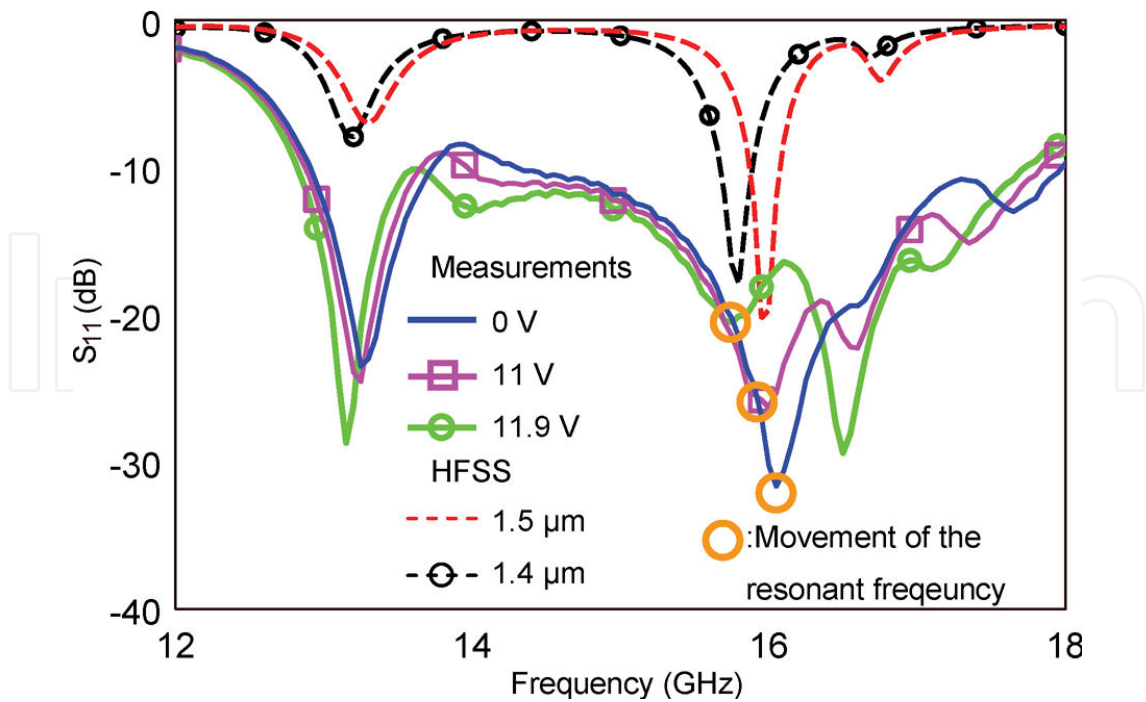
Figure 13. |S$_{11}$|parameters for different actuation voltages and simulation results [14]

Discrete frequency tuning can be illustrated with a reconfigurable annular slot antenna with a monolithic integration of MEMS actuators presented by B.A. Cetiner in [15]. The architecture and a photograph of the microstrip-fed reconfigurable antenna annular slot are shown in Figure 14. The antenna has two concentric circular slots. According to MEMS switch S$_1$ state, they can be individually excited in order to achieve frequency reconfigurability. S$_2$ and S$_3$ switches enable the metallic annular ring, which stays between the outer and inner slots, to be shorted to RF ground.

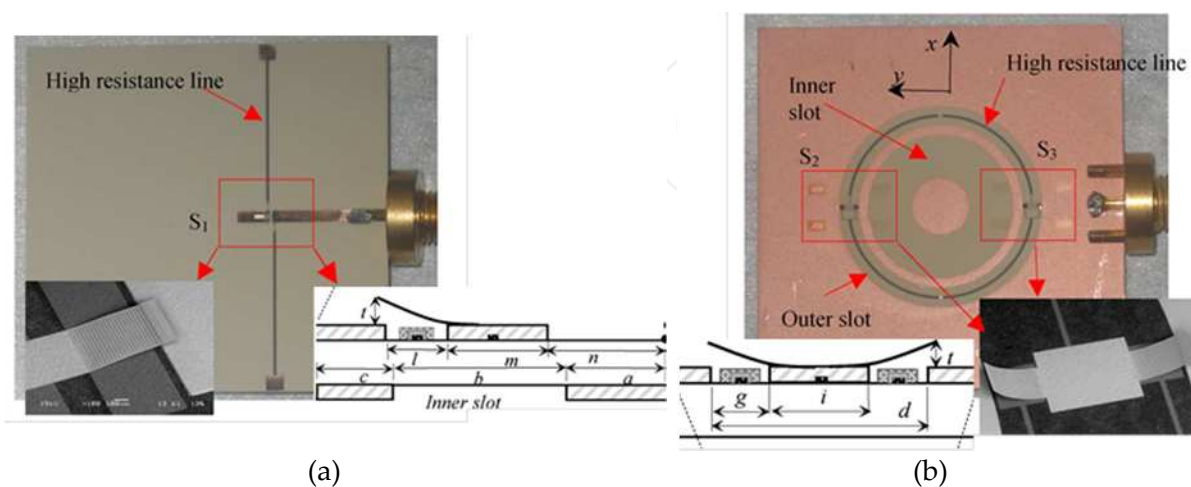(a)   (b)

Figure 14. Microstrip feeding line integrating a single-arm MEMS switch (a) and the annular slot integrating two double-arm MEMS actuators [15]

The measured $|S_{11}|$ parameters (Figure 15) show that when MEMS switches are activated (down-state) by applying DC bias voltages, the antenna working band is around 5.2 GHz. Vice-versa, when MEMS switches are in the up-state, the antenna is working at 2.4 GHz.
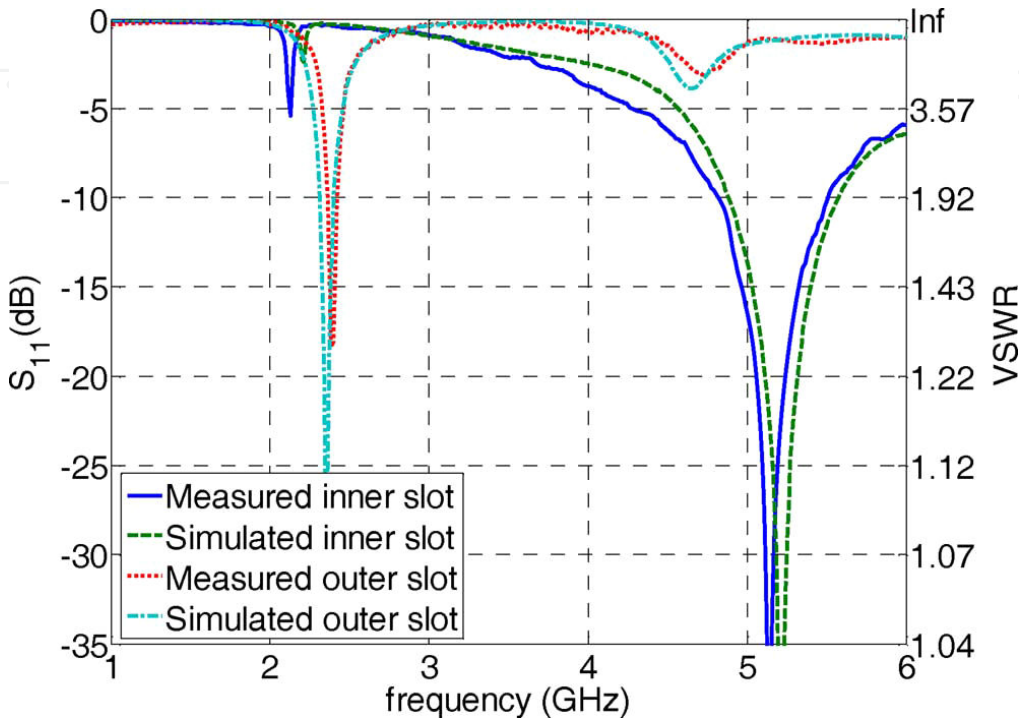

Figure 15. Measured and simulated $|S_{11}|$parameters for MEMS switches activated (5.2 GHz) and deactivated (2.4 GHz) [15]

2.1.4. Field Effect Transistor

Continuous frequency tuning can be achieved by using Field Effect Transistor. In [16], S. Kawasaki presents a slot antenna loaded with two one-port reactive FET. The electrically length of the slot is changing according to the voltage bias applying on the FET. The measured $|S_{11}|$ parameters (see Figure 16) show a 10% frequency tuning range for a gate tuning voltage (V_{gs}) going from 0V to-0.6V while the drain voltage (V_{ds}) is tuned from 0V to 0.4V.

2.2. Agile antennas using tunable materials

Changing the material characteristics in a part of antenna designs also promise the ability to tune them in frequency. The application of a static electric field can be used to change the relative permittivity of a ferroelectric material or a liquid crystal, respectively a static magnetic field can changed the relative permeability of a ferrite. In case of printed antennas, these changes modify the effective electrical length of antennas, and then resulting in shifts of their operating frequencies.
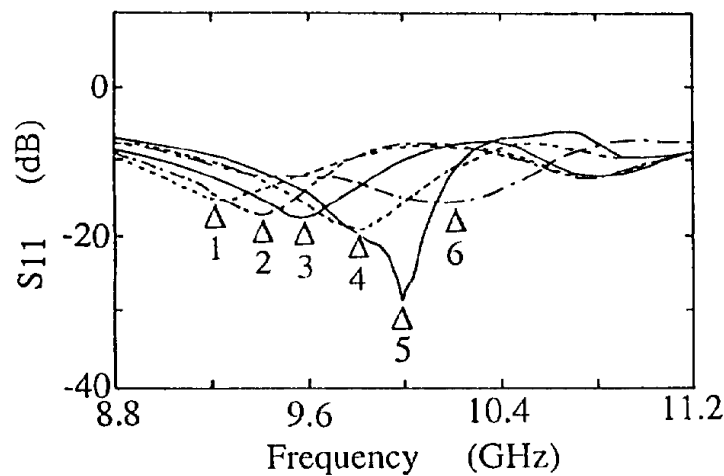
Figure 16. Measured $|S_{11}|$ parameters for both gate and drain tuning voltages [16]

2.2.1. Ferroelectric materials

Lead-based perovskite ceramics such as $PbZr_xTi_{1-x}O_3$ (PZT) have been the leaders, for the past 50 years, on ferroelectric material research [17] for electronic devices, sensors, actuators, and medical ultrasonic transducers, owing to their good dielectric properties over a wide temperature range. Due to health care and environmental regulations, restriction of hazardous substances as lead has been required [18]. Since the last 10 years, many efforts have been mainly devoted in the field of microwave applications to $Ba_xSr_{1-x}TiO_3$ (BST) material which is one of the most attractive materials [19] because it presents high dielectric constant, relatively low dielectric loss, interesting tunability and small temperature dependence. In fact, in BST, the Curie temperature (Tc) which defines the ferroelectric/paraelectric transition is tuned by controlling the Ba/Sr ratio. More recently some other ferroelectric ceramics such as the tantalate niobate oxide $KTa_xNb_{1-x}O_3$ (KTN) or the sodium bismuth titanate $Na_{0.5}Bi_{0.5}TiO_3$ (BNT) and its solid solutions BNT-BT are emerging.

Two different methods exist to polarize a ferroelectric material with a static electric field. A better tunability is obtained when the static electric field is perpendicular to the two electrodes. For antenna application point of view, antenna designs integrating ferroelectric materials have to move toward this kind of polarization in order to have a better reconfigurability. However, many efforts have to be devoted from realization and also simulation point of views. Therefore, compact antenna community exhibits only few papers of this kind of antennas.

V. K. Palukuru et al. [20] present a tunable antenna using an integrated ferroelectric-thick film made of BST material. The antenna is depicted in Figure 17. It exhibits a folded slot antenna loading with a BST thin film varactor. In order to tune the dielectric permittivity of the BST film, a DC bias voltage is applied thanks to a bias-T component, which was attached to the Vector Network Analyzer. The BST varactor is placed over the radiating slot: the upper electrode (0.2 mm 0.2 mm) is part of the antenna's metallization and the lower electrode is the antenna's ground plane. In order to reduce the capacitance of the varactor, a slight horizontal

offset is used between the electrodes. Therefore, the electric field for biasing the material is both in the vertical and the horizontal directions.
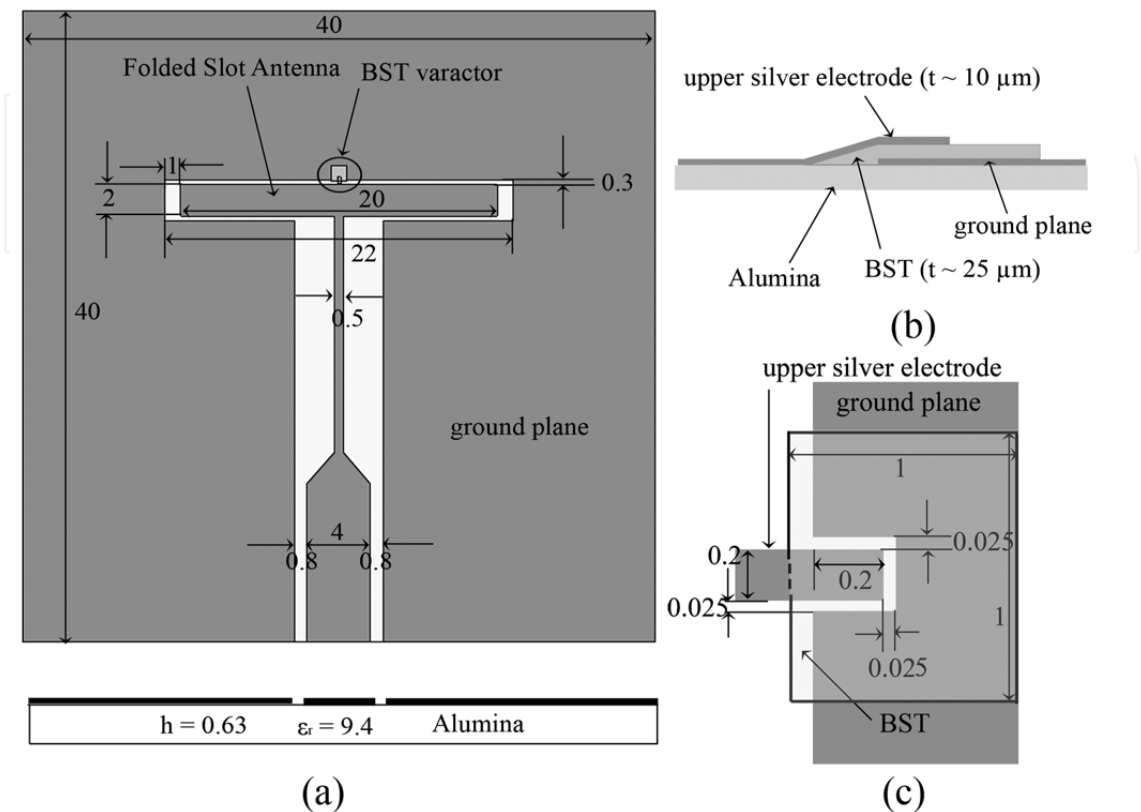

Figure 17. Folded slot antenna with the BST varactor (a), side cross-section (b) and top view (c) of the BST varactor [20]

The $|S_{11}|$ parameters (Figure 18) show that a frequency tunability of 3.5% can be obtained with a change of the bias voltage from 0V to 200V.
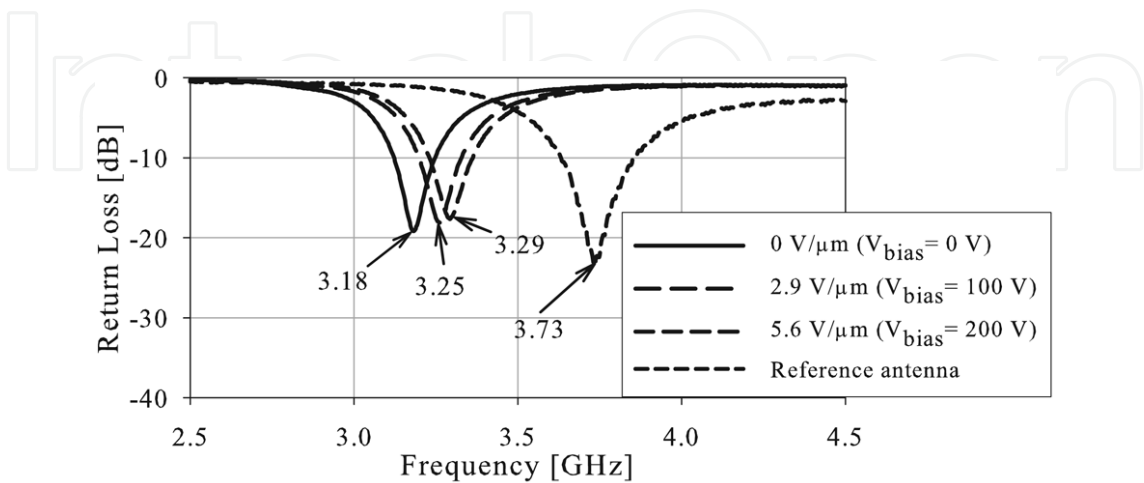

Figure 18. Measured $|S_{11}|$ parameters for different DC-bias voltages [20]

H. Jiang presents a coplanar waveguide (CPW) square-ring slot antenna as showed Figure 19 [21]. Nine shunt ferroelectric BST thin film varactors are integrated with the CPW antenna structure achieving both antenna miniaturization and reconfiguration.
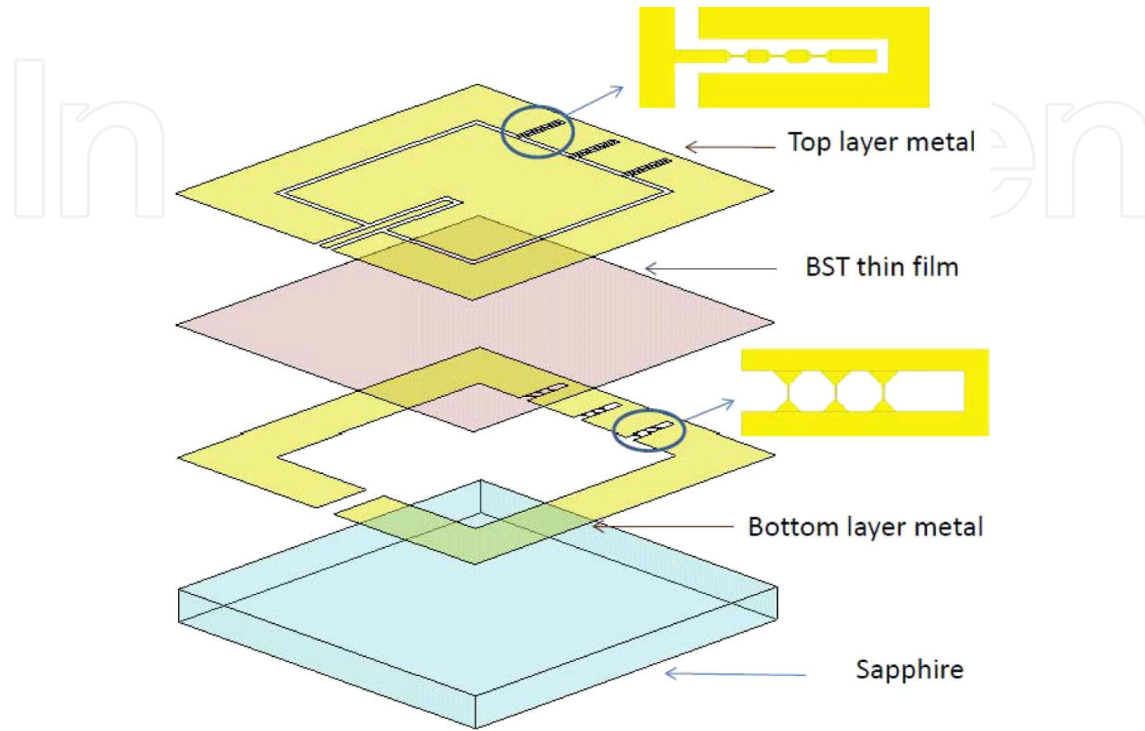

Figure 19. Coplanar waveguide square-ring slot antenna integrating BST material [21]

Figure 20 shows the measured $|S_{11}|$ parameter with DC bias voltages from 0 V to 7 V. Therefore the antenna working band is continuously tuned from 5.28 GHz up to 5.77 GHz.

2.2.2. Liquid crystal

Another technological approach for designing an agile antenna is the use of liquid crystal as a tunable dielectric. Indeed, the characterizations of liquid crystals [22-24] have shown that they are promising tunable materials for microwave applications, especially for operating frequencies above 10 GHz. The material features low dielectric loss and continuous tunability with low bias power consumption. The literature show that some microwave applications are using liquid crystals, e.g. for polarization agile antenna [25], tunable patch antennas [26], reflectarrays [27-28], filters [29], resonators [30] and variable delay lines [31-33].

In this framework, L. Liu presents in [34] a tunable patch antenna using a liquid crystal. Its operating frequency is around 5 GHz with a tuning range around 4% in measurement. The Figure 21 presents the antenna geometry composed of three layers of Taconic substrate. The liquid crystal is injected in the middle layer just under the microstrip patch and between the ground plane and patch top hat. A DC bias voltage was applied between the patch and ground across the liquid crystal using a bias tee at the feed input.

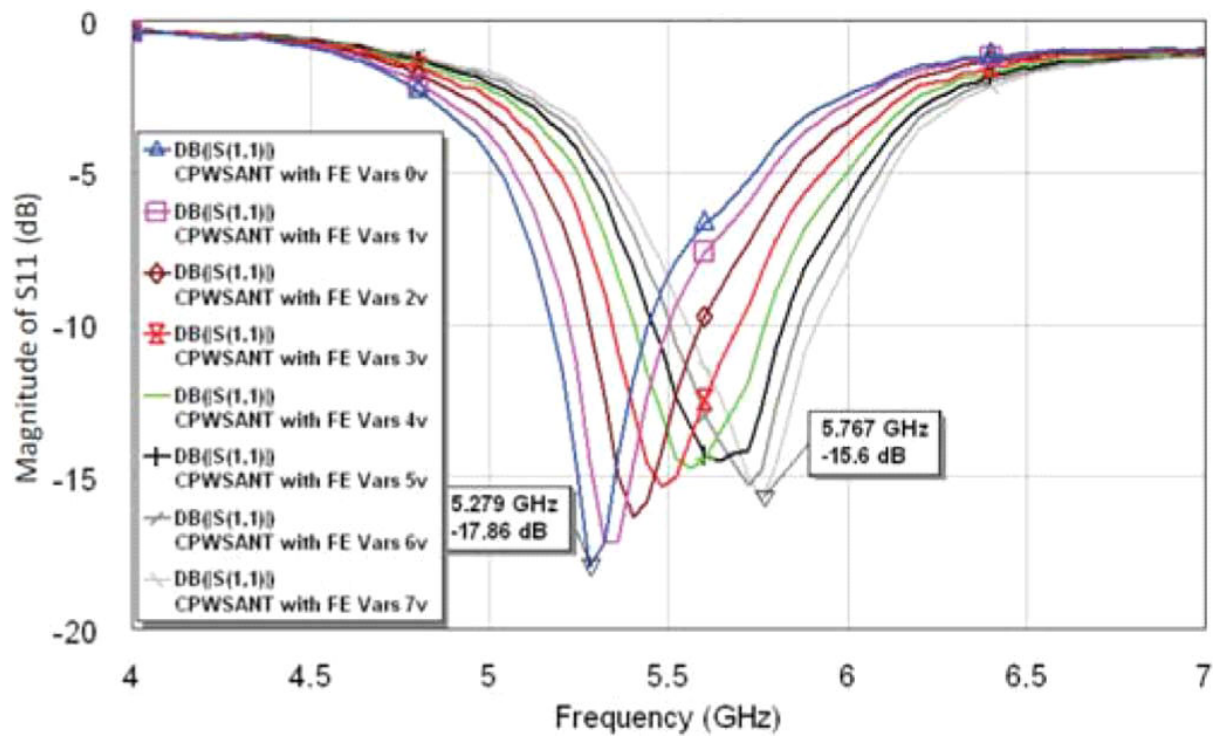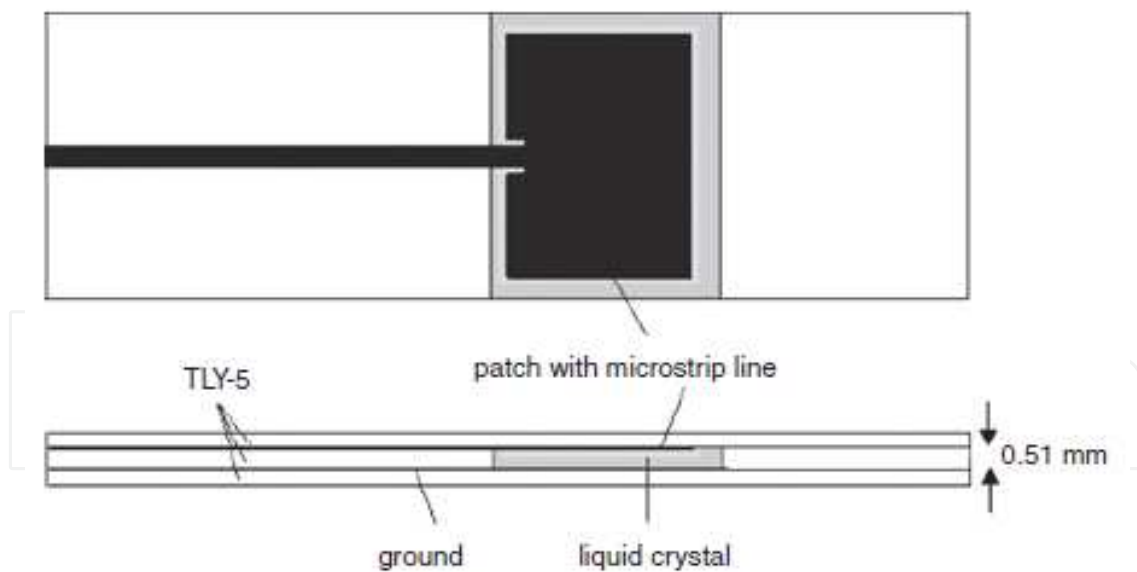**Figure 20.** Measured |S$_{11}$|parameters for different DC-bias voltages [21]

Figure 21. Tunable patch antenna using a liquid crystal [34]

The Figure 22 shows the measured return losses for the patch antenna for three states of liquid crystal bias: 0V, 5V and 10V. The 0V state reveals that the used liquid crystal without DC bias presents somewhat high losses around 0.12 for the loss tangent. Thus a 4% frequency tuning

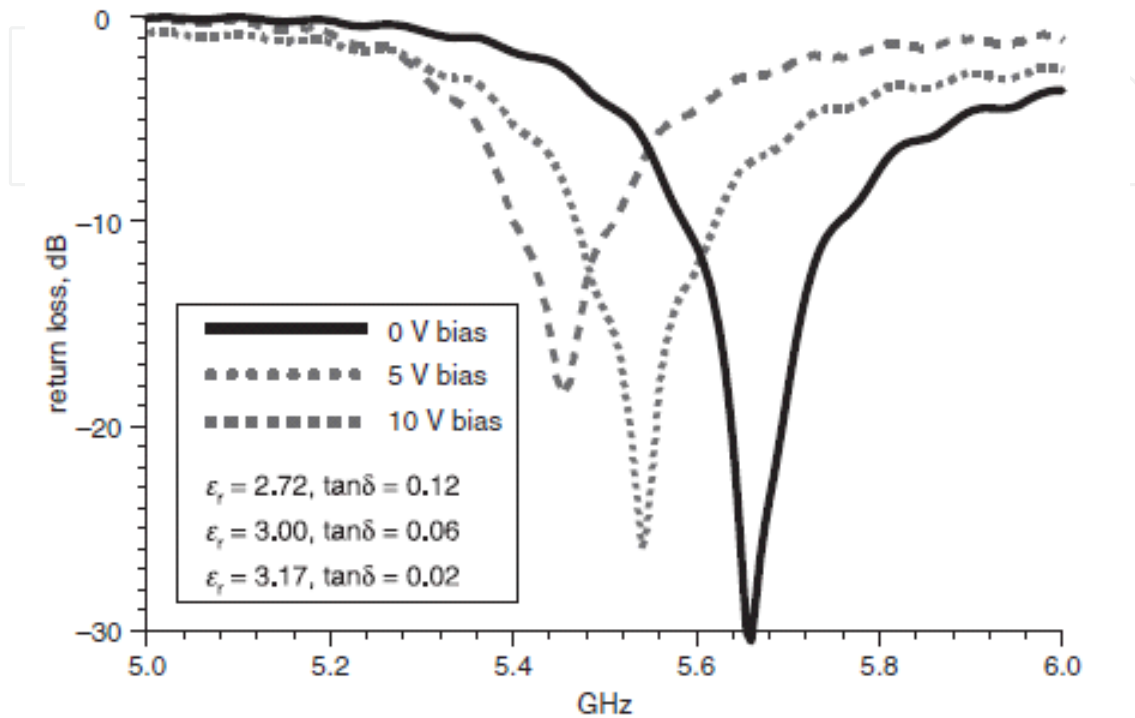can be achieved with relatively poor radiation efficiencies, i.e. 14% at least (at 0V) to 40% (at 10V).

Figure 22. Measured $|S_{11}|$ parameters for different DC-bias voltages [34]

2.2.3. Ferrite materials

Frequency-tuned ferrite-based antennas are rarely presented in the literature. In [35] and [36], authors study patch antennas on ferrite substrates (Figure 23) whereas A. Petosa presents in [37] a ferrite resonator antenna. In this latter, biasing of the ferrite with a static magnetic field is achieved using a permanent magnet. The magnet was located under the ferrite antenna beneath the ground plane. For a parallel magnetic-bias orientation, the resonance frequency can be tuned on 8% of bandwidth. That scales to 9% for a perpendicular magnetic-bias orientation.

All results presented in the literature and investigated the properties of ferrite-based microstrip antennas indicate that factors including non-uniform bias fields and the multiple modal field distributions excited in a bulk ferrite substrate may preclude their use in practical applications.

Now that an overview of the most common used techniques for compact antennas to become active has been presented, the next part will address both challenges and how to integrate active components in order to maximize the antenna performances and efficiency.
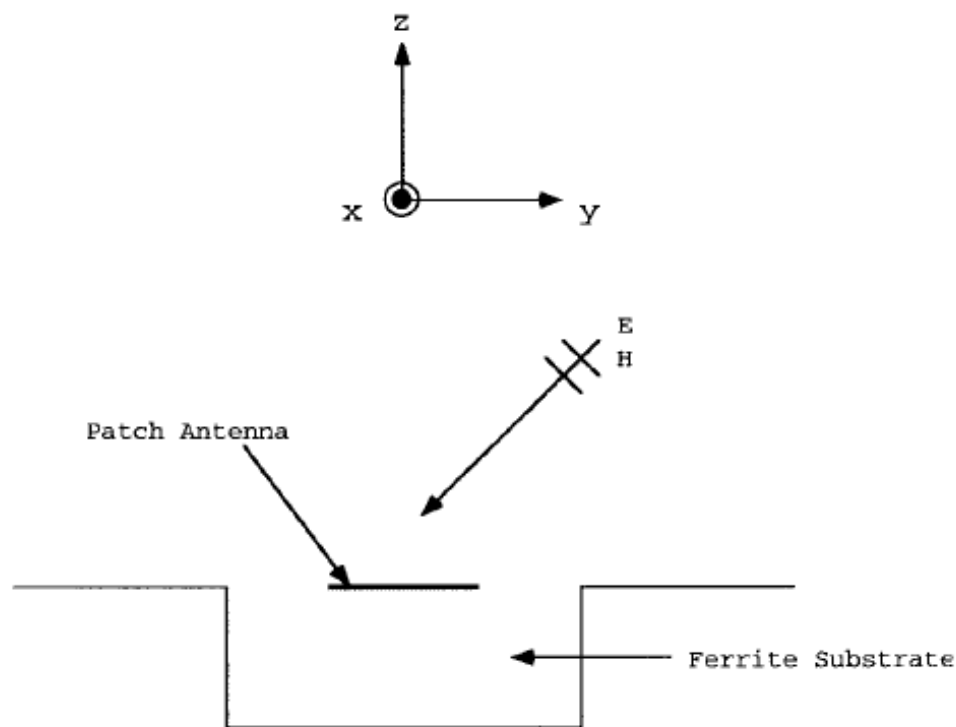
Figure 23. Patch antenna on a ferrite substrate [37]

3. Relevant parameter for frequency agile antenna studies – New approach for wireless applications.

3.1. How to integrate an active component – Challenges

To implement the reconfigurability in an antenna, the knowledge of the active component or the tunable material is essential. Even in case of commercial components, as varactor or PIN diodes, users and particularly the microwave community do not have enough parameters and information at RF frequencies. Some papers detail the integration of the RF equivalent circuit of the used component [10],[13].

The varactor diodes integrated in an antenna for frequency reconfigurability is the most popular way. Thus, this section will focus on varactor diodes issues. However, arguments can be extended to other frequency tuning methods.

In [10], the paper completes the lack of information related to most of varactor diode data-sheets. Indeed, constructor only provide characteristics at low frequencies and do not give enough parameters for antenna application point of view, such as capacitance values, serial resistance and accepted power at RF frequencies. The chosen varactor in this paper has been characterized according to antenna designer criteria and its electromagnetic model has been deduced. This example is chosen in the framework of this chapter.

To correctly explain this example, the next subsection will investigate the place where the varactor can be integrated. Following the presentation of the varactor diode manufacturer's

datasheet, a complete characterization meeting antenna designer's criteria will be explained. That will lead to the determination of the varactor diode S parameters. With the knowledge of the latter, two methods will be explained and described to reach an accurate antenna simulation and realization:

- The electromagnetic equivalent circuit of the varactor diode can be deduced from the S parameters thanks to Agilent ADS.

- The S parameters of the varactor diode can be directly injected in the electromagnetic simulator CST Microwave Studio® and the antenna performances deduced thanks to a co-simulation.

3.1.1. Varactor diode area in an antenna

The varactor diode is a tunable capacitor which loads the antenna in order to artificially increase its electrical length. To be the most efficient, it must be placed where the electrical field is maximum. Take a folded Inverted F Antenna for example presented Figure 24. The maximum of the electrical field is at the end of the radiating element (see Figure 24). To be integrated at this place and joined the ground plane at the same time, the varactor diode can be soldered between the ribbon and the ground. In most cases, DC-block capacitors have to be added for the varactor's DC-bias not to be shunt.
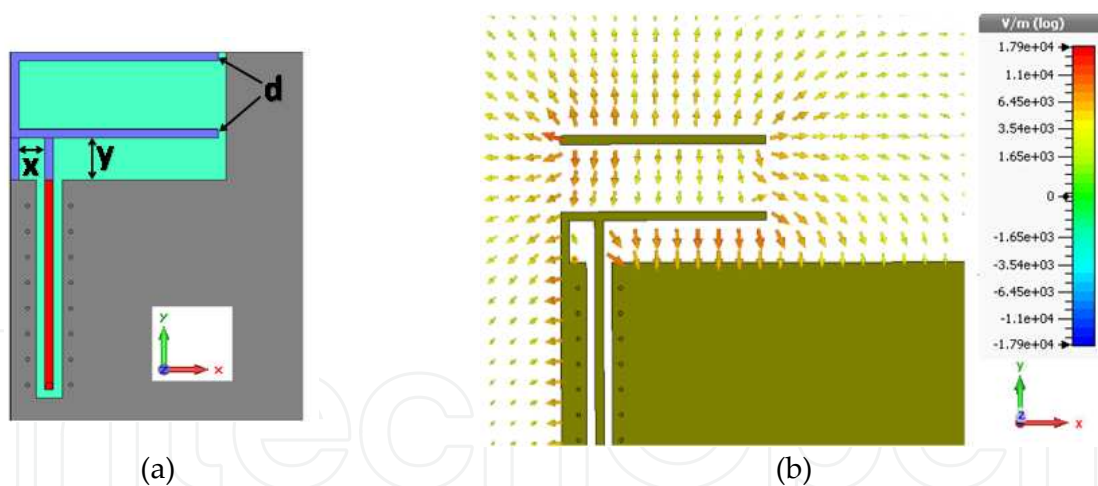

(a)   (b)

Figure 24. Inverted F Antenna Measured (a) and the total electric field on the radiating element (b)

3.1.2. Varactor diode datasheet

In [10], the chosen GaAs hyperabrupt varactor diode MGV125-22 (Aeroflex Metelics) [38] has a capacity range between 0.2 pF and 2 pF for 0 to 22 Volts tuning voltage as shown Figure 25. However, these values are given as a rough line and the datasheet does not give enough parameters for high frequencies antenna application's point of view. Indeed, the values for junction capacitance C_j (Figure 25) and the quality factor Q are supplied by the manufacturer

and are almost always specified at a low frequency. The Figure 25 shows the widely used varactor diode model with L_p and C_p the values of the package inductance and capacitance.
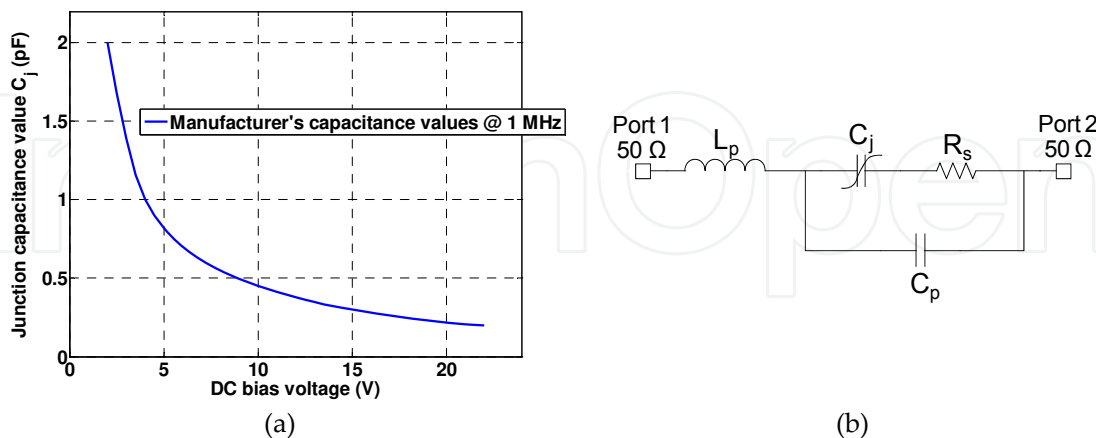

Figure 25. Manufacturer's capacitance value (extracted at 1MHz) versus the DC bias voltage (a) and the Varactor di-ode model (b)

In the MGV125-22 case, junction capacitance values are specified at 1 MHz and the Q factor equals 3000 at 50 MHz for a DC bias voltage of –4 Volts. Q is defined by $Q=1/(\omega C_j R_s)$. This formula can be used to calculate the series resistance R_s of the varactor model at the measured frequency, its value is assumed to be constant with reverse voltage. Thus, at 50 MHz $R_s=1.06\Omega$. It is important to note that R_s impacts directly the antenna total efficiency. A too high value (from 3Ω) is basically penalizing for antenna performances. This enhances the need to assess its value at microwave frequencies. For this purpose, the hyperabrupt varactor diode has to be characterized close to operating conditions (here between 470 MHz and 862 MHz).

3.1.3. Varactor diode characterization

• First method: Electromagnetic model

The varactor diode is soldered on a 50 Ω impedance microstrip line as shown Figure 26. A dedicated TRL (Through-Reflect-Line) calibration kit is manufactured (Figure 26) in order to de-embed both connectors and lines. Thus S parameters of the single varactor diode can be deduced. Considering the varactor diode model previously presented in Figure 26, C_j, L_p, C_p and R_s values can be deduced for each voltage and for a constant injected power of-10 dBm. Therefore, model component values are adjusted (see Figure 26) in order their S parameters to correspond with the measured ones. The Figure 26 shows the comparison between S parameters of the determined electromagnetic model (Agilent ADS) and the measured ones for 2 Volts and 10 Volts DC bias voltages.

These results are given as an example and the same work has been done for varactor reverse bias voltages varying from 2V to 22V with a 2V step. As expected, the corresponding electro-magnetic model presents constant values according to the DC bias voltage (Figure 27):
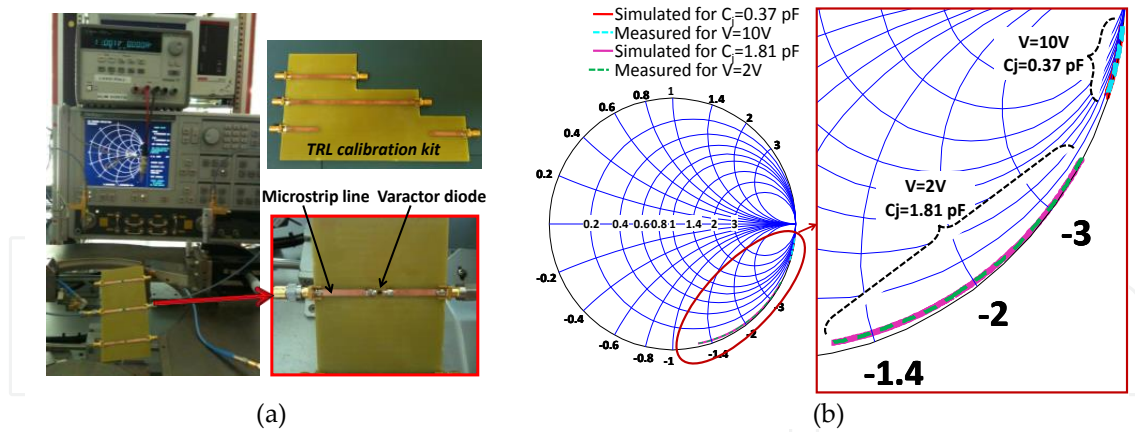
Figure 26. Characterization of the varactor diode (a) and the Comparison between the electromagnetic model and the measurement on S_{11} parameter on the [400 MHz – 1 GHz] frequency band (b)

L_p=3.821nH, C_p=0.08pF and R_s=1.8Ω. The C_j value presented in Figure 27 decreases as a function of DC bias voltage value.
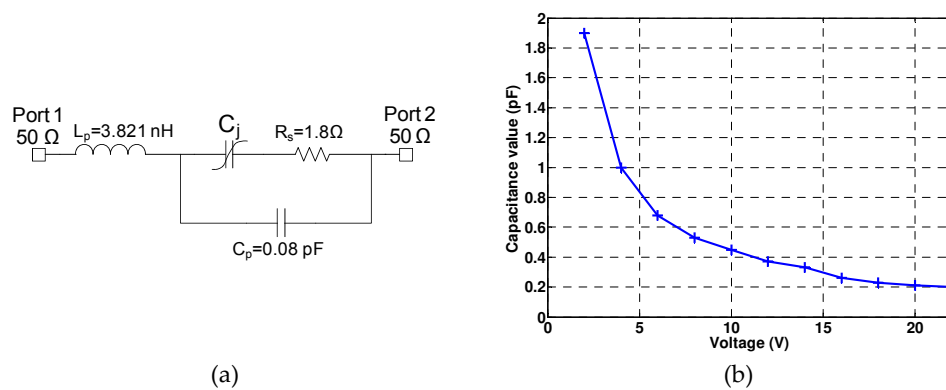

Figure 27. Electromagnetic model with the capacitance values C_j versus the DC bias voltage (b)

• Second method: Co-simulation

Another way is to directly insert the S parameters touchstone file of the varactor diode in the antenna electromagnetic simulation as illustrated in Figure 28.
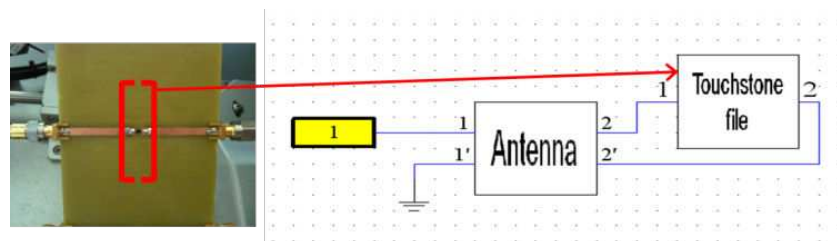

Figure 28. Co-simulation of the antenna including measured S parameters of the diode

Thanks to the previous TRL calibration, only the varactor diode S parameters are inserted in the simulator. By this way, both antenna and varactor diode are combined and the S parameters of the global device can be directly simulated. An example (presented paragraph 3.3) will confirm that the two previous methods exhibit similar antenna performances.

3.2. Limitations of currently varactor diode method – Power characterization

Figure 29 provides some information regarding the accepted power by the varactor diode: high injected power involves some varactor diode distortions.
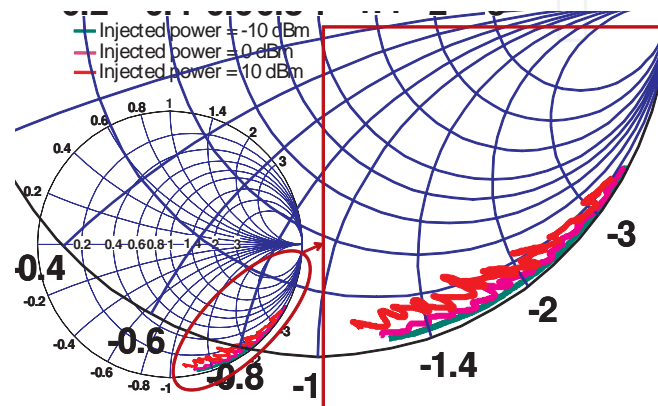

Figure 29. Measured S parameters according to the injected power

This figure presents S parameters of the diode for only three values of injected power:-10 dBm, 0 dBm and 10 dBm. The non-linear distortion of the diode has been studied. It reveals that the varactor diode model well fits measurements for an injected RF power lower than-5 dBm. Beyond this injected power (see for 0 dBm), no varactor model can fit the measurement. Regarding antenna's parameters, the following example will show that a large RF power (upper than-5 dBm) involves a mismatched antenna. As far as the DVB-H application, the system is only working in receiving mode, the diode distortion will never appear and the linear electromagnetic model can be used and integrated in the electromagnetic simulator. Indeed, for receiver devices, the antenna accepted power is far lower than – 5 dBm.

3.3. Example of a basic tunable DVB-H antenna

This subsection investigates an example to show the interest of the previous varactor diode characterization. This was briefly presented in [4], it is completed here by adding the first method (electromagnetic model) and the power characterization. A basic IFA prototype loaded by the same varactor diode (see Figure 30) has been manufactured.

It has been measured for a-10 dBm RF power and its performances compared with three simulations: with both presented methods and with the varactor diode's datasheet (Figure 31). $|S_{11}|$ parameters show that both investigated methods and measurement present a good agreement. Moreover, they are different from $|S_{11}|$ parameters determined with the varactor diode datasheet. That underlines the relevance of the varactor diode characterization. Regard-
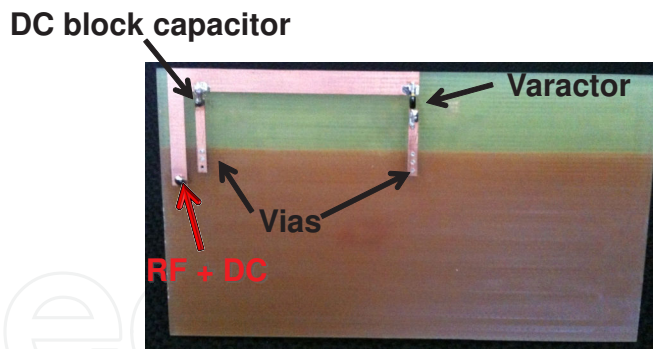
Figure 30. Basic IFA prototype

ing the antenna total efficiency, it equals 50% in the real case whereas it reaches 60% when the varactor datasheet is used in electromagnetic simulations.

Power characterization is illustrated on Figure 31. This figure reminds the measured $|S_{11}|$ parameter for a power of-10 dBm. For a 10 dBm injected power, the measured $|S_{11}|$ parameter is compared with the simulated one with the second method.
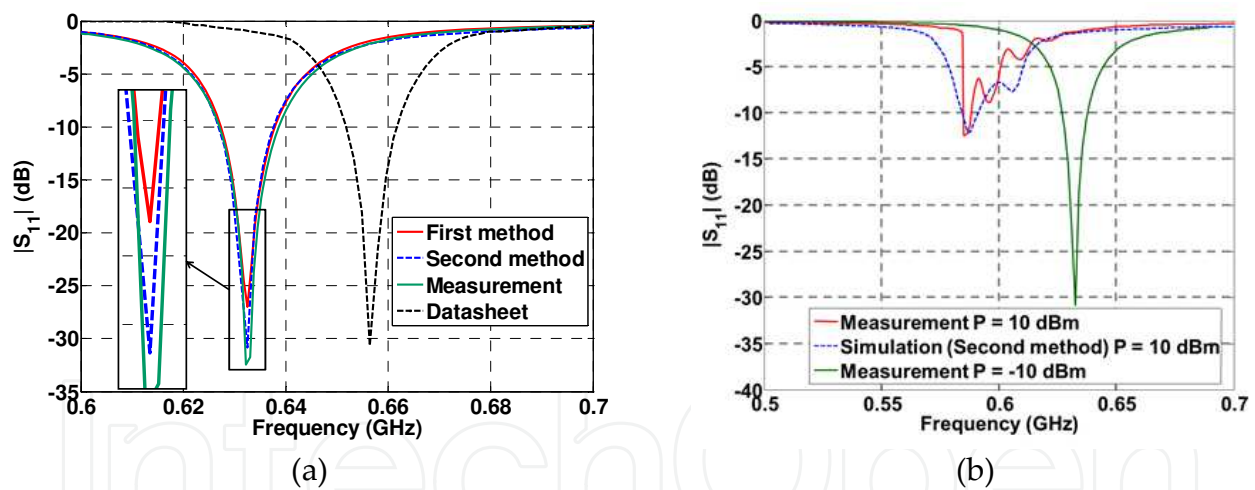
Figure 31. $|S_{11}|$ parameters for the different methods (a) and according to the injected power (b)

There is a good agreement between the measurement and the simulation. This figure shows that the non-linearity of the varactor diode disturbs the $|S_{11}|$ parameter of the antenna. Thus, this kind of varactor diode has to be used only for reception devices.

Therefore, this section has presented how to integrate and characterize a varactor diode. It reveals the importance of the diode characterization in a design flow dedicated to antenna structure.

3.4. Discussion and trade-offs between agility techniques and physical limitations

According to the aimed application, trade-offs are necessary to design a frequency tunable antenna.

- For discrete frequency tuning, PIN diodes or MEMS switches can be planed.

- For continuous frequency tuning, which is often aiming for compact antennas, varactor diodes, MEMS variable capacitor and tunable materials can be used.

However, previous paragraphs have revealed that varactor diodes are not usable for transmitter devices because of their non-linearity for considering power levels.

The RF characterization of ferroelectric films shows high power handling capability [39]. Good permittivity tunability may be obtained if both materials properties and variable capacitor sizes have been properly dimensioned. The conclusion is the same for MEMS variable capacitor.

Studies on both ferroelectric material and MEMS capacitor merit extended investigations because these solutions seem to be the best and most promising alternatives faced with varactor diodes.

Performing rigorous full-wave analysis of these new components is the new challenge to extract their accurate electromagnetic models. Antennas would be optimized by considering the real response of these components. These investigations would enable the co-development of antennas integrating components' electromagnetic models.

4. Conclusion

To conclude, an overview of compact and frequency agile antenna has been presented and detailed in this chapter while mentioning a lot of literature references. A special part has been dedicated to the presentation of the most common method to achieve a frequency tuning: the use of varactor diodes. Their integration within an antenna to be the most efficient has been shown. The study exhibits varactor diodes characterization and also reveals their limitation. A summary of the presented methods according to the intended application has been presented. Eventually, some ideas on varator diodes alternatives have been proposed in order to make antenna tunability viable for transmitter devices.

Author details

L. Huitema and T. Monediere

University of Limoges, Xlim Laboratory, France

References

[1] Huitema, L.; Sufyar, S.; Delaveaud, C.; D'Errico, R., "Miniature antenna effect on the ear-to-ear radio channel characteristics," *Antennas and Propagation (EUCAP), 2012 6th European Conference on*, vol., no., pp.3402,3406, 26-30 March 2012

[2] Libo Huang; et al., "Electrically Tunable Antenna Design Procedure for Mobile Applications," *Microwave Theory and Techniques, IEEE Transactions on*, vol.56, pp. 2789-2797, Dec. 2008

[3] Li, Y., Zhang, Z., Chen, W., Feng, Z. and Iskander, M. F. (2010), A compact DVB-H antenna with varactor-tuned matching circuit. Microw. Opt. Technol. Lett., 52: 1786–1789

[4] Huitema, L.; Reveyrand, T. et al., "A compact and reconfigurable DVB-H antenna for mobile handheld devices," *Antennas and Propagation (EUCAP), Proceedings of the 5th European Conference on*, vol., no., pp.1314-1317, 11-15 April 2011

[5] Canneva, F.; Ribero, J.; Staraj, R., "Tunable antenna for DVB-H band," *Antennas and Propagation (EuCAP), 2010 Proceedings of the Fourth European Conference on*, vol., no., pp.1,3, 12-16 April 2010

[6] Bhartia, P.; Bahl, I.J., "A frequency agile microstrip antenna," *Antennas and Propagation Society International Symposium, 1982*, vol.20, no., pp.304,307, May 1982

[7] Erfani, E.; Nourinia, J.; Ghobadi, C.; Niroo-Jazi, M.; Denidni, T.A., "Design and Implementation of an Integrated UWB/Reconfigurable-Slot Antenna for Cognitive Radio Applications," *Antennas and Wireless Propagation Letters, IEEE*, vol.11, no., pp. 77,80, 2012

[8] Behdad, N.; Sarabandi, K., "A varactor-tuned dual-band slot antenna," *Antennas and Propagation, IEEE Transactions on*, vol.54, no.2, pp.401,408, Feb. 2006

[9] Behdad, N.; Sarabandi, K., "Dual-band reconfigurable antenna with a very wide tunability range," *Antennas and Propagation, IEEE Transactions on*, vol.54, no.2, pp.409,416, Feb. 2006

[10] Huitema, L.; Reveyrand, T.; Mattei, J.-L.; Arnaud, E.; Decroze, C.; Monediere, T., "Frequency Tunable Antenna Using a Magneto-Dielectric Material for DVB-H Application," *Antennas and Propagation, IEEE Transactions on*, vol.61, no.9, pp.4456,4466, Sept. 2013

[11] Laheurte, J.-M., "Switchable CPW-fed slot antenna for multifrequency operation," *Electronics Letters*, vol.37, no.25, pp.1498,1500, 6 Dec 2001

[12] Outi Kivekäs, Jani Ollikainen, and Pertti Vainikainen, "Frequency-tunable internal antenna for mobile phones", 12th International Symposium on Antennas (JINA 2002). Nice, France, 12-14 November 2002, volume 2, pages 53-56

[13] Peroulis, D.; Sarabandi, K.; Katehi, L. P B, "Design of reconfigurable slot antennas," *Antennas and Propagation, IEEE Transactions on*, vol.53, no.2, pp.645,654, Feb. 2005

[14] Erdil, Emre; Topalli, K.; Unlu, M.; Civi, O.A.; Akin, T., "Frequency Tunable Microstrip Patch Antenna Using RF MEMS Technology," *Antennas and Propagation, IEEE Transactions on*, vol.55, no.4, pp.1193,1196, April 2007

[15] Cetiner, B.A.; Crusats, G.R.; Jofre, L.; Biyikli, Necmi, "RF MEMS Integrated Frequency Reconfigurable Annular Slot Antenna," *Antennas and Propagation, IEEE Transactions on*, vol.58, no.3, pp.626,632, March 2010

[16] Kawasaki, S.; Itoh, T., "A slot antenna with electronically tunable length," *Antennas and Propagation Society International Symposium, 1991. AP-S. Digest*, vol., no., pp. 130,133 vol.1, 24-28 June 1991

[17] N. Setter, D. Damjanovic, et al., Ferroelectric thin films: Review of materials, properties, and applications, J. Appl. Phys. 100, (2006)

[18] P. K. Panda, Review: environmental friendly lead-free piezoelectric materials, J. Mater. Sci. 44, 5049–5062, (2009)

[19] A. K.Tagantsev, V. O. Sherman, K. F. Afanasiev, J. Venkatesh and N. Setter, Ferroelectric Materials for Microwave Tunable Applications, J. Electroceram., 11, 5-66, 2003

[20] Palukuru, V.K.; Komulainen, M.; Tick, T.; Perantie, J.; Jantunen, Heli, "Low-Sintering-Temperature Ferroelectric-Thick Films: RF Properties and an Application in a Frequency-Tunable Folded Slot Antenna," *Antennas and Wireless Propagation Letters, IEEE*, vol.7, no., pp.461,464, 2008

[21] Hai Jiang; Patterson, M.; Brown, D.; Chenhao Zhang; KuanChang Pan; Subramanyam, G.; Kuhl, D.; Leedy, K.; Cerny, C., "Miniaturized and Reconfigurable CPW Square-Ring Slot Antenna Loaded With Ferroelectric BST Thin Film Varactors," *Antennas and Propagation, IEEE Transactions on*, vol.60, no.7, pp.3111,3119, July 2012

[22] Schaub, D.E.; Oliver, D.R., "A Circular Patch Resonator for the Measurement of Microwave Permittivity of Nematic Liquid Crystal," *Microwave Theory and Techniques, IEEE Transactions on*, vol.59, no.7, pp.1855,1862, July 2011

[23] Mueller, S.; Penirschke, A.; Damm, C.; Scheele, P.; Wittek, M.; Weil, Carsten; Jakoby, R., "Broad-band microwave characterization of liquid crystals using a temperature-controlled coaxial transmission line," *Microwave Theory and Techniques, IEEE Transactions on*, vol.53, no.6, pp.1937,1945, June 2005

[24] Bulja, S.; Mirshekar-Syahkal, D.; James, R.; Day, S.E.; Fernandez, F.A., "Measurement of Dielectric Properties of Nematic Liquid Crystals at Millimeter Wavelength," *Microwave Theory and Techniques, IEEE Transactions on*, vol.58, no.12, pp.3493,3501, Dec. 2010

[25] Karabey, O.H.; Bildik, S.; Bausch, S.; Strunck, S.; Gaebler, A.; Jakoby, R., "Continuously Polarization Agile Antenna by Using Liquid Crystal-Based Tunable Variable Delay Lines," *Antennas and Propagation, IEEE Transactions on*, vol.61, no.1, pp.70,76, Jan. 2013

[26] Luyi Liu; Langley, R., "Electrically small antenna tuning techniques," *Antennas & Propagation Conference, 2009. LAPC 2009. Loughborough*, vol., no., pp.313,316, 16-17 Nov. 2009

[27] Wenfei Hu; Arrebola, M.; Cahill, R.; Encinar, J.A.; Fusco, V.; Gamble, H.S.; Alvarez, Y.; Las-Heras, F., "94 GHz Dual-Reflector Antenna With Reflectarray Subreflector," *Antennas and Propagation, IEEE Transactions on*, vol.57, no.10, pp.3043,3050, Oct. 2009

[28] Yazdanpanahi, M.; Bulja, S.; Mirshekar-Syahkal, D.; James, R.; Day, S.E.; Fernandez, F.A., "Liquid-crystal-based mm-wave tunable resonator," *Microwave Conference (EuMC), 2010 European*, vol., no., pp.1233,1236, 28-30 Sept. 2010S.P.; Grant, N., "Phase agile reflectarray cells based on liquid crystals," *Microwaves, Antennas & Propagation, IET*, vol.1, no.4, pp.809,814, Aug. 2007

[29] Goelden, F.; Gaebler, A.; Karabey, O.; Goebel, M.; Manabe, A.; Jakoby, R., "Tunable band-pass filter based on Liquid Crystal," *German Microwave Conference, 2010*, vol., no., pp.98,101, 15-17 March 2010

[30] Yazdanpanahi, M.; Bulja, S.; Mirshekar-Syahkal, D.; James, R.; Day, S.E.; Fernandez, F.A., "Liquid-crystal-based mm-wave tunable resonator," *Microwave Conference (EuMC), 2010 European*, vol., no., pp.1233,1236, 28-30 Sept. 2010

[31] Kuki, T.; Fujikake, H.; Nomoto, T., "Microwave variable delay line using dual-frequency switching-mode liquid crystal," *Microwave Theory and Techniques, IEEE Transactions on*, vol.50, no.11, pp.2604,2609, Nov 2002

[32] Goelden, F.; Gaebler, A.; Goebel, M.; Manabe, A.; Mueller, S.; Jakoby, R., "Tunable liquid crystal phase shifter for microwave frequencies," *Electronics Letters*, vol.45, no. 13, pp.686,687, June 18 2009

[33] Karabey, O.H.; Goelden, F.; Gaebler, A.; Strunck, S.; Jakoby, R., "Tunable loaded line phase shifters for microwave applications," *Microwave Symposium Digest (MTT), 2011 IEEE MTT-S International*, vol., no., pp.1,1, 5-10 June 2011

[34] Liu, L.; Langley, R.J., "Liquid crystal tunable microstrip patch antenna," *Electronics Letters*, vol.44, no.20, pp.1179,1180, September 25 2008

[35] Brown, A.D.; Volakis, J.L.; Kempel, Leo C.; Botros, Y.Y., "Patch antennas on ferromagnetic substrates," *Antennas and Propagation, IEEE Transactions on*, vol.47, no.1, pp. 26,32, Jan 1999

[36] Mishra, R.K.; Pattnaik, S.S.; Das, N., "Tuning of microstrip antenna on ferrite substrate," *Antennas and Propagation, IEEE Transactions on*, vol.41, no.2, pp.230,233, Feb 1993

[37] Petosa, A.; Mongia, R.K.; Cuhaci, M.; Wight, J.S., "Magnetically tunable ferrite reso-nator antenna," *Electronics Letters*, vol.30, no.13, pp.1021,1022, 23 Jun 1994

[38] *Aeroflex Metelics datasheet*, Available: http://www.aeroflex.com/AMS/Metelics/pdfiles/MGV_Series_Hyperabrupt_A17041.pdf

[39] Laur, V.; Costes, R.; Houndonougbo, F.; et al., "Microwave study of tunable planar capacitors using mn-doped $ba_{0.6}sr_{0.4}tio_3$ ceramics," *Ultrasonics, Ferroelectrics and Fre-quency Control, IEEE Transactions on*, vol.56, no.11, pp.2363-2369, November 2009